Collective band structures in the odd-proton nuclei ^{135,137}Pm

C. W. Beausang, L. Hildingsson,* E. S. Paul, W. F. Piel, Jr., P. K. Weng,† N. Xu, and D. B. Fossan

Physics Department, State University of New York at Stony Brook, Stony Brook, New York 11794

(Received 21 April 1987)

Collective bands based on a low-K $\pi h_{11/2}$ orbital have been populated to high spins in the odd-proton nuclei ^{135,137}Pm following the reactions ^{116}Sn(^{24}Mg,p4n)^{135}Pm and ^{114}Cd(^{27}Al,4n)^{137}Pm, respectively. Both nuclei exhibit a band crossing in the $\pi h_{11/2}$ band at a frequency of $\hbar\omega \sim 0.42$ MeV. In ^{135}Pm, an upbend is observed, while a weaker interaction backbend is observed in ^{137}Pm. Cranked-shell model calculations, including triaxiality, imply that this crossing is due to the alignment of the second and third valence $h_{11/2}$ protons. The systematics of this alignment in the Pm isotopes will be discussed. In addition, positive parity three-quasiproton states were observed in both nuclei. These structures also contain a pair of aligned $h_{11/2}$ protons, in this case the first and second valence protons which align at a much lower frequency of $\hbar\omega \sim 0.28$ MeV.

I. INTRODUCTION

In the light rare-earth nuclei around mass $A = 135$ the proton Fermi surface lies near the bottom of the $h_{11/2}$ shell. Odd-proton nuclei therefore exhibit rotational bands built on these low-K $h_{11/2}$ intruder levels. Such bands show a maximal signature splitting; only one signature component $(\alpha = -\frac{1}{2})$ of the band, consisting of stretched $\Delta J = 2$ transitions, is observed experimentally. The magnitude of the signature splitting is known[1] to depend on the nuclear shape parameter γ, namely the degree of triaxiality. Although the nuclei in this region exhibit relatively flat potential energy surfaces[2,3] with respect to γ, the $h_{11/2}$ quasiproton orbitals stabilize a near-axial prolate deformation $(\gamma \sim 0°)$. The odd-proton occupying an $h_{11/2}$ orbital also blocks the lowest frequency $(\hbar\omega \sim 0.3$ MeV$)$ alignment of the first pair of valence $h_{11/2}$ protons. The higher frequency alignments $(\hbar\omega \sim 0.45$ MeV$)$ observed in these bands may then be due to the alignment of the second and third valence $h_{11/2}$ protons, maintaining a near-prolate deformation of the nucleus, or alternatively by the alignment of the first pair of valence $h_{11/2}$ neutrons. Such an alignment of neutrons in high-K orbitals from the upper $h_{11/2}$ midshell is expected to force the nuclear shape towards $\gamma \sim -60°$ which, in the Lund convention,[4] represents the collective rotation of an oblate shape around an axis perpendicular to the symmetry axis. For near-prolate $(\gamma \sim 0°)$ shapes, cranked shell-model (CSM) calculations predict the alignment of the $h_{11/2}$ protons (second and third) to occur at a lower frequency than the alignment of the $h_{11/2}$ neutrons (first pair).

Whether the observed alignments in the yrast bands of odd-proton nuclei in this mass region are caused by protons or neutrons depends strongly on the ease with which the nucleus can be changed from a prolate $(\gamma = 0°)$ to an oblate $(\gamma = -60°)$ shape, i.e., the prolate-oblate energy difference. If the oblate shape lies at an excitation energy of less than 300 keV with respect to the prolate shape, it is expected that the neutron alignment can compete with the proton alignment. Such is the case[5-7] in the odd-proton nuclei ^{131}La $(Z = 57)$,

^{133}Pr $(Z = 59)$, and more recently ^{139}Pm $(Z = 61)$, where collective oblate $(\gamma \sim -60°)$ bands have been observed built on the $\pi h_{11/2} \otimes (vh_{11/2})^2$ configuration. These collective bands coexist with near-prolate rotational bands built on quasiproton configurations. Similarly there is increasing evidence for the coexistence of prolate proton-aligned bands and oblate neutron-aligned bands in several neighboring even-even nuclei, for example ^{134,136}Nd (Refs. 8 and 9) and ^{138}Sm, which have recently been studied in this laboratory. Furthermore, other even-even nuclei in this region are known to possess isomeric 10^+ states built on the $(vh_{11/2})^2$ configuration, for example ^{134}Ce (Ref. 10) and the $N = 78$ isotones[11] ^{136}Ce, ^{138}Nd, and ^{140}Sm. However, for the ^{135,137}Pm isotopes the prolate-oblate energy difference is estimated to be somewhat higher,[2,12] thus suppressing the competition of neutron alignment.

A comparison will be made of the $\pi h_{11/2}$ band crossings observed in the $Z = 61$ isotopes ^{133,135,137,139}Pm. The nucleus ^{133}Pm was studied in this laboratory using the ^{110}Cd(^{28}Si,p4n)^{133}Pm reaction, and has also been reported by Lister et al.[13] Preliminary results for ^{135,137}Pm have been presented previously.[14,15] The nucleus ^{139}Pm was studied[7] using the ^{116}Cd(^{27}Al,4n)^{139}Pm reaction.

II. EXPERIMENTAL PROCEDURES AND RESULTS

States in ^{135}Pm were populated using the ^{116}Sn(^{24}Mg, p4n)^{135}Pm reaction at a bombarding energy of 144 MeV, while the ^{114}Cd(^{27}Al,4n)^{137}Pm reaction at 131 MeV was used to populate states in ^{137}Pm. The heavy-ion beams were delivered by the Stony Brook Superconducting LINAC injected by the tandem Van de Graaff accelerator. The tin target consisted of 2 mg/cm^2 of ^{116}Sn rolled onto a ^{208}Pb backing of thickness 50 mg/cm^2 which served to stop the recoils and the beam. The cadium target consisted of 3.3 mg/cm^2 of ^{114}Cd rolled onto a ^{208}Pb backing of thickness 110 mg/cm^2.

The data reported here included γ-ray excitation functions, angular distributions, and γ-γ coincidence measurements. In order to decide on the optimum bombard-

ing energy for each reaction, γ-ray singles spectra were recorded as a function of bombarding energy. In addition to ^{135}Pm (p4n), the ^{24}Mg + ^{116}Sn reaction also produced significant amounts of ^{135}Nd (2p3n) and ^{136}Pm (p3n); the ^{27}Al + ^{114}Cd reaction also produced ^{136}Nd (p4n) and ^{134}Pr (α3n) in addition to ^{137}Pm (4n).

The γ-γ coincidence data were recorded using four n-type Ge detectors, each having an efficiency of 25% relative to a 7.6 cm × 7.6 cm NaI(Tl) detector for 1.3 MeV γ rays. The detectors were located at ±57° and ±136° with respect to the beam direction, and at a distance of 14 cm from the target. Each of the four detectors utilized bismuth germanate (BGO) anti-Compton shields of the transverse type.[16] The coincidence data were recorded onto magnetic tape event-by-event for subsequent data analysis. A total of approximately 30 million coincidence events were recorded for both the ^{24}Mg + ^{116}Sn reaction and the ^{27}Al + ^{114}Cd reaction.

The tapes were scanned off-line on a VAX 11-780 computer to produce a symmetrized 2048×2048 array of E_γ vs E_γ. Background-subtracted gated spectra were generated from this array and were used in the construction of the decay schemes of ^{135,137}Pm shown in Figs. 1 and 2, respectively. Figures 3 and 4 display examples of gated coincidence spectra from the ^{24}Mg + ^{116}Sn and ^{27}Al + ^{114}Cd data, respectively.

Separate experiments were performed to obtain angular distribution information for the transitions assigned to ^{135,137}Pm; these made use of the reactions ^{112}Cd(^{27}Al, 4n)^{135}Pm at 141 MeV and ^{114}Cd(^{27}Al,4n)^{137}Pm at 129 MeV, respectively. In each case, one Compton-suppressed Ge counter was positioned successively at each of four angles with respect to the beam axis, namely 90°, 120°, 135°, and 152°. A Ge(Li) detector, placed at −90°, was used as a monitor.

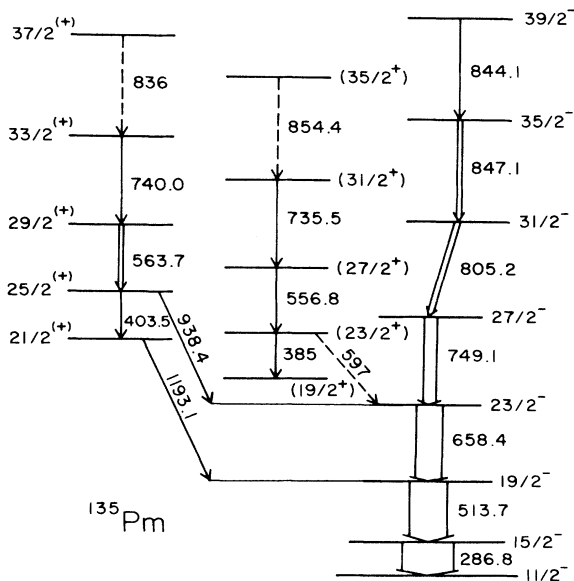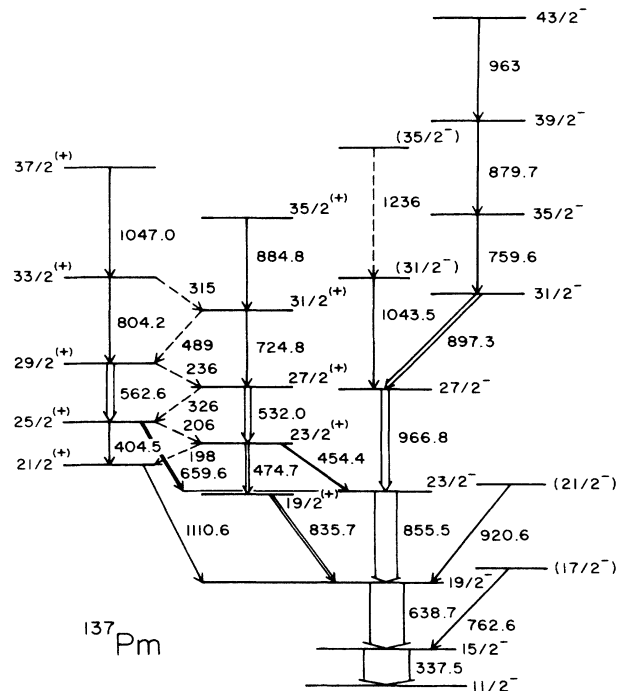In order to obtain information about the multipolarity

FIG. 2. The proposed level scheme of ^{137}Pm deduced from this work. The transition energies are given in keV and the widths of the arrows indicate their intensities.

of the transitions observed in the two nuclei ^{135,137}Pm, the formula

$$W(\theta) = A_0 + A_2 P_2(\theta) + A_4 P_4(\theta) \qquad (1)$$

was fitted to the empirical γ-ray intensity function $W(\theta)$, where θ is the angle of the detector relative to the beam axis; A_0, A_2, and A_4 are adjustable parameters; while $P_2(\theta)$ and $P_4(\theta)$ are Legendre polynomials. The results for ^{135,137}Pm are listed in Tables I and II, respec-

FIG. 1. The proposed level scheme of ^{135}Pm deduced from this work. The transition energies are given in keV and the widths of the arrows indicate their intensities.
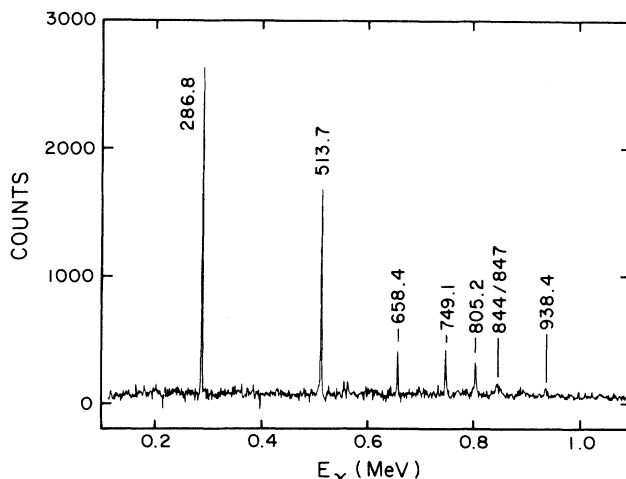

FIG. 3. A sum of gated coincidence spectra set on the 658.4 and 749.1 keV transitions in ^{135}Pm. The energies of the labeled peaks are given in keV.
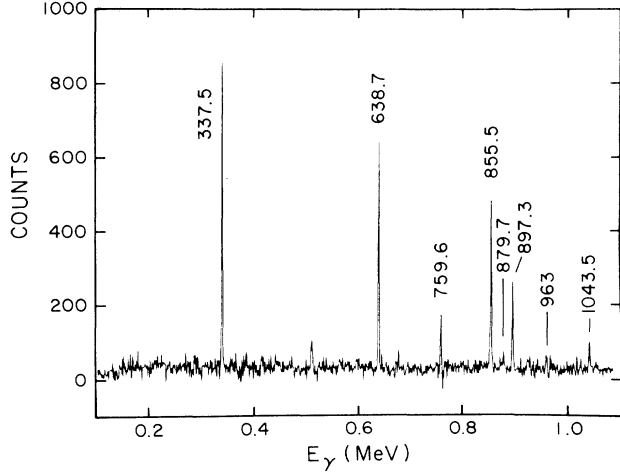
FIG. 4. A gated coincidence spectrum set on the 966.8 keV transition in ^{137}Pm. The energies of the labeled peaks are given in keV.

tively, where a small correction has been made to each A_2/A_0 and A_4/A_0 ratio for the finite detector size. Because of numerous unresolved doublets and weak transition intensities, most of the intensities listed in Tables I and II were determined from the γ-γ coincidence data. These intensity values have been corrected for the efficiency of the Ge detectors and normalized to

the $\frac{15}{2}^- \rightarrow \frac{11}{2}^-$ transitions at the bottom of the $\pi h_{11/2}$ bands in the two nuclei ^{135}Pm and ^{137}Pm, respectively.

III. DISCUSSION

Experimental alignments[17]

$$i_x = I_x - I_{x,\text{ref}} \tag{2}$$

of the bands observed in ^{135,137}Pm are shown in Fig. 5 (full lines). Here, I_x is the projection of the total spin onto the rotation axis defined semiclassically as

$$I_x = [(I + \tfrac{1}{2})^2 - K^2]^{1/2} \tag{3}$$

and $I_{x,\text{ref}}$ is a reference based on a frequency-dependent moment of inertia, i.e.,

$$I_{x,\text{ref}} = \omega \mathcal{J}_{\text{ref}} = \omega(\mathcal{J}_0 + \omega^2 \mathcal{J}_1) . \tag{4}$$

The Harris[18] parameters were taken as $\mathcal{J}_0 = 12.5\hbar^2$ MeV^{-1} and $\mathcal{J}_1 = 16\hbar^4$ MeV^{-3}.

Figures 6 and 7 show CSM calculations for one- and three-quasiparticle Routhians plotted as a function of the γ deformation and at a fixed rotational frequency of $\hbar\omega = 250$ keV. The deformation parameters were taken as $\epsilon_2 = 0.2$ and $\epsilon_4 = 0.0$; the proton and neutron pairing strengths were set equal at $\Delta_p = \Delta_n = 1.2$ MeV; and the proton and neutron Fermi energies, λ_p and λ_n, were chosen to reproduce the particle numbers $Z = 61$ and $N = 74$. Cranked shell-model calculations are relatively insensitive to the exact values of these parameters. As

TABLE I. Gamma-ray energies, intensities, angular distribution data, and tentative spin and parity assignments for ^{135}Pm. Except where indicated, the intensities were obtained from coincidence data.

E_γ (keV)	I_γ	A_2/A_0	A_4/A_0	Assignment
286.8 (1)	≡100[a]	+0.140(14)	−0.053(20)	$\frac{15}{2}^- \rightarrow \frac{11}{2}^-$
385(1)	<1			$\frac{23}{2}^+ \rightarrow \frac{19}{2}^+$
403.5(1)	5.7(4)	+0.501(65)	−0.150(91)	$\frac{25}{2}^+ \rightarrow \frac{21}{2}^+$
513.7(1)	83.7(1.2)			$\frac{19}{2}^- \rightarrow \frac{15}{2}^-$
556.8(1)	3.1(5)			$\frac{27}{2}^+ \rightarrow \frac{23}{2}^+$
563.7(2)	7.5(6)			$\frac{29}{2}^+ \rightarrow \frac{25}{2}^+$
597(1)	<1			$\frac{23}{2}^+ \rightarrow \frac{23}{2}^-$
658.4(2)	62.8(1.1)[a]	+0.223(20)	−0.050(27)	$\frac{23}{2}^- \rightarrow \frac{19}{2}^-$
735.5(2)	3.8(5)			$\frac{31}{2}^+ \rightarrow \frac{27}{2}^+$
740.0(3)	3.8(6)			$\frac{33}{2}^+ \rightarrow \frac{29}{2}^+$
749.1(1)	27.5(9)	+0.151(31)	−0.025(44)	$\frac{27}{2}^- \rightarrow \frac{23}{2}^-$
805.2(2)	17.7(9)			$\frac{31}{2}^- \rightarrow \frac{27}{2}^-$
836(1)	<1			$\frac{37}{2}^+ \rightarrow \frac{33}{2}^+$
844.1(9)	5.8(1.3)			$\frac{39}{2}^- \rightarrow \frac{35}{2}^-$
847.1(4)	11.7(9)			$\frac{35}{2}^- \rightarrow \frac{31}{2}^-$
854.4(6)	<1			$\frac{35}{2}^+ \rightarrow \frac{31}{2}^+$
938.4(3)	5.5(7)	b		$\frac{25}{2}^+ \rightarrow \frac{23}{2}^-$
1193.1(2)	4.9(7)[a]	−0.071(73)	−0.13(10)	$\frac{21}{2}^+ \rightarrow \frac{19}{2}^-$

[a]Intensity obtained from angular distribution data.
[b]Unresolved doublet.

seen, the results are very sensitive to the value of the shape asymmetry γ. The definition of γ is taken to be consistent with the Lund convention.[4] The shape of the nucleus and sense of rotation are shown at the top of Fig. 6 for specific values of γ that correspond to axially symmetric shapes. These calculations will be discussed in more detail in the following sections.

A. The $\pi h_{11/2}$ yrast bands of ^{135,137}Pm

In both ^{135}Pm and ^{137}Pm the yrast bands are based on the signature $\alpha = -\frac{1}{2}$ component of the $[541]\frac{3}{2}^-$ Nilsson orbital derived from the $h_{11/2}$ shell. Nilsson single-particle systematics at a quadrupole deformation $\epsilon_2 = 0.2$ were used to assign this level in both nuclei. The odd

proton in the $h_{11/2}$ orbital favors a triaxial shape for the nucleus with $\gamma \sim -15°$, as shown in Fig. 6. An upbend is evident in the alignment plot for the yrast band of ^{135}Pm, shown in Fig. 5, at a rotational frequency of $\hbar\omega = 0.42$ MeV, while a backbend is observed at the same frequency in the corresponding plot for ^{137}Pm. Similarly, band crossings are also observed at $\hbar\omega \sim 0.42$ MeV in the corresponding bands of the ^{133}Pm and ^{139}Pm isotopes; the alignment plots for these nuclei are also included in Fig. 5 (dashed lines). The crossing in ^{133}Pm is seen as a smooth upbend, whereas that seen in ^{135}Pm is a sharp upbend, and finally backbends are observed in both ^{137}Pm and ^{139}Pm. The progression of the band crossing from an upbend to a backbend in the ^{133,135,137,139}Pm isotopes is due to a decreasing interaction between the one- and three-

TABLE II. Gamma-ray energies, intensities, angular distribution data, and tentative spin and parity assignments for ^{137}Pm. Except where indicated, the intensities were obtained from coincidence data.

E_γ (keV)	I_γ	A_2/A_0	A_4/A_0	Assignment
199.0(5)	<1			$\frac{23}{2}^+ \to \frac{21}{2}^+$
205.5(5)	<1			$\frac{25}{2}^+ \to \frac{23}{2}^+$
236.0(5)	<1			$\frac{29}{2}^+ \to \frac{27}{2}^+$
315(1)	<1			$\frac{33}{2}^+ \to \frac{31}{2}^+$
326.0(5)	<1			$\frac{27}{2}^+ \to \frac{25}{2}^+$
337.5(1)	$\equiv 100.0^a$	+0.314(30)	−0.005(30)	$\frac{15}{2}^- \to \frac{11}{2}^-$
404.5(1)	6.1(4)	+0.386(82)	0.00(12)	$\frac{25}{2}^+ \to \frac{21}{2}^+$
454.4(1)	$7.4(3)^a$	+0.480(98)	−0.05(10)	$\frac{23}{2}^+ \to \frac{23}{2}^-$
474.7(1)	8.4(5)	+0.130(47)	−0.094(66)	$\frac{23}{2}^+ \to \frac{19}{2}^+$
489.0(6)	<1			$\frac{31}{2}^+ \to \frac{29}{2}^+$
532.0(1)	13.0(5)	+0.229(51)	+0.582(68)	$\frac{27}{2}^+ \to \frac{23}{2}^+$
562.6(1)	12.7(5)			$\frac{29}{2}^+ \to \frac{25}{2}^+$
638.7(1)	72.4(8)	b		$\frac{19}{2}^- \to \frac{15}{2}^-$
659.6(1)	8.4(5)	−0.028(74)	+0.09(10)	$\frac{25}{2}^+ \to \frac{23}{2}^-$
724.8(2)	6.4(6)			$\frac{31}{2}^+ \to \frac{27}{2}^+$
759.6(2)	4.4(6)			$\frac{35}{2}^- \to \frac{31}{2}^-$
762.6(2)	3.4(3)			$\frac{17}{2}^- \to \frac{15}{2}^-$
804.2(2)	6.0(5)			$\frac{33}{2}^+ \to \frac{29}{2}^+$
835.7(1)	11.4(6)	+0.33(12)	+0.18(18)	$\frac{19}{2}^+ \to \frac{19}{2}^-$
855.5(1)	$46.3(5)^a$	+0.338(22)	+0.025(34)	$\frac{23}{2}^- \to \frac{19}{2}^-$
879.7(4)	1.5(5)			$\frac{39}{2}^- \to \frac{35}{2}^-$
884.8(4)	1.8(6)			$\frac{35}{2}^+ \to \frac{31}{2}^+$
897.3(2)	$8.8(3)^a$	+0.22(10)	0.00(13)	$\frac{31}{2}^- \to \frac{27}{2}^-$
920.6(3)	2.3(5)			$\frac{21}{2}^- \to \frac{19}{2}^-$
962.5(5)	1.7(5)			$\frac{43}{2}^- \to \frac{39}{2}^-$
966.8(1)	$17.0(5)^a$	+0.192(63)	+0.017(98)	$\frac{27}{2}^- \to \frac{23}{2}^-$
1043.5(2)	3.0(7)			$\frac{31}{2}^- \to \frac{27}{2}^-$
1047.0(5)	2.2(8)			$\frac{37}{2}^+ \to \frac{33}{2}^+$
1110.6(1)	6.4(7)	−0.227(48)	+0.126(72)	$\frac{21}{2}^+ \to \frac{19}{2}^-$
1236(1)	<1			$\frac{35}{2}^- \to \frac{31}{2}^-$

[a]Intensity obtained from angular distribution data.
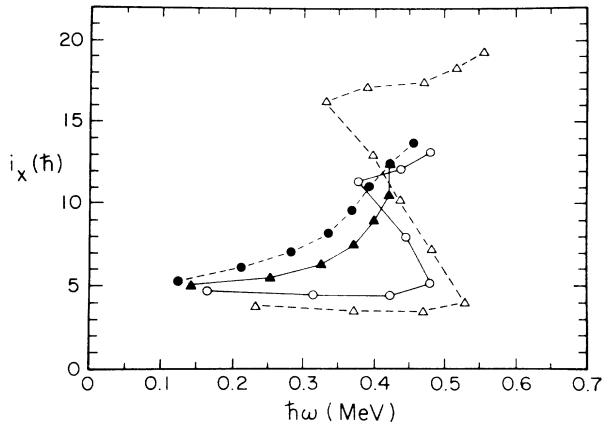[b]Doublet with $4^+ \to 2^+$ transition in ^{134}Ce.

FIG. 5. The experimental alignment i_x of the bands in ^{133}Pm (full circles), ^{135}Pm (full triangles), ^{137}Pm (open circles), and ^{139}Pm (open triangles) shown as a function of rotational frequency.

FIG. 7. Total Routhians of single and multiquasiparticle states calculated as a function of the γ deformation. The calculations were performed at $\hbar\omega = 250$ keV and assume that the energies of the axially symmetric prolate ($\gamma = 0°$) and oblate ($\gamma = -60°$) shapes are degenerate, i.e., $V_{po} = 0$.

quasiparticle bands as the neutron number increases. The transitions of energies 1043 and 1236 keV, shown above the $\frac{27}{2}^-$ state in the level scheme of ^{137}Pm, may be the continuation of the one-quasiproton $\pi h_{11/2}$ band. These states are observed due to the weak interaction between the one- and three-quasiproton bands. The decreasing quadrupole deformation ϵ_2 with increasing mass number may contribute towards this observed difference in the interaction strengths in the promethium isotopes.

The valence quasiparticle orbitals from a high-j shell exert strong γ-driving forces on the nuclear core. The γ deformation for which the orbital Routhian is minimized changes smoothly from $\gamma = +60°$ (oblate noncollective) to $\gamma = -120°$ (prolate noncollective) as the Fermi surface rises through the shell.[19] For the proton Fermi surface appropriate to the promethium isotopes, the valence
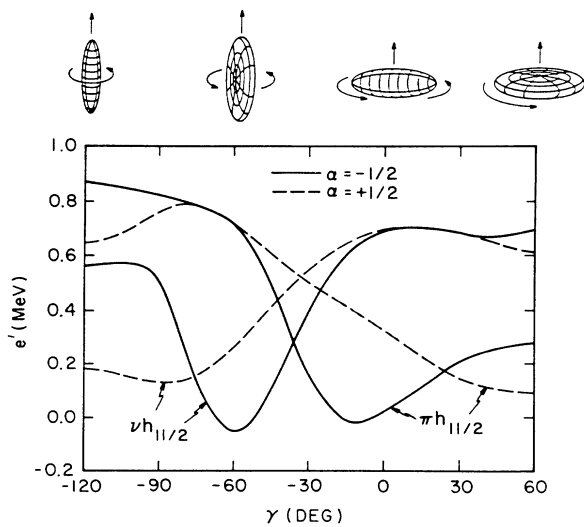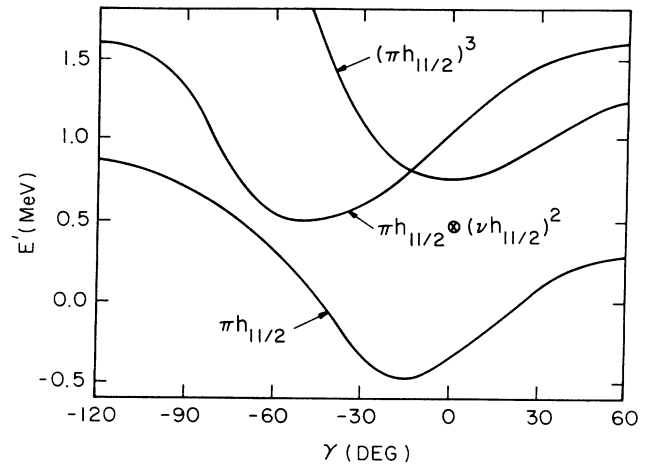
quasiproton orbitals favor a triaxial shape with $\gamma \sim -15°$, as can be seen in Fig. 6. Therefore, although the nuclei in this region are γ soft, the odd proton occupying such a quasiparticle orbital will stabilize the nucleus at this deformation.

The measured crossing frequencies in these nuclei are in good agreement with CSM calculations for the alignment of the second and third valence $h_{11/2}$ protons, with $\gamma = -15°$. The low frequency alignment ($\hbar\omega \sim 0.3$ MeV) of the first pair of valence $h_{11/2}$ protons is blocked in these bands due to the presence of the odd proton. The two transitions of energies 763 and 921 keV feeding into the yrast band of ^{137}Pm at the levels of spin $\frac{15}{2}^-$ and $\frac{19}{2}^-$, respectively, may connect the yrast band (signature $\alpha = -\frac{1}{2}$) with the band built on the unfavored signature ($\alpha = +\frac{1}{2}$) component of the $\pi h_{11/2}$ orbital. The signature splitting between the two components, extracted from experimental Routhians, is approximately 500 keV; this value is consistent with the maximal splitting that occurs at $\gamma \sim -15°$, as can be seen from Fig. 6. The alignment of the additional $h_{11/2}$ quasiprotons will provide an additional driving force stabilizing the nuclear shape at this value of γ.

At this value of $\gamma = -15°$, the alignment of the first pair of valence $h_{11/2}$ neutrons is also calculated to occur at a frequency similar to that of the protons. However, an alignment of the neutrons would tend to drive the nuclear shape towards $\gamma \sim -60°$, which represents a collectively rotating oblate shape. For this shape the signature splitting of the $h_{11/2}$ proton orbital is small (see Fig. 6) leading to the observation of a $\Delta J = 1$ band based on the $\pi h_{11/2} \otimes (\nu h_{11/2})^2$ configuration. Such bands have been observed[5,6] in ^{131}La and ^{133}Pr. If the nucleus is sufficiently "stiff" with respect to this shape change in the γ plane, the neutron alignment will be hindered.

Hence, whereas the alignment of $h_{11/2}$ protons favors a near-prolate triaxial shape ($\gamma \sim -15°$), the alignment of

FIG. 6. Calculated proton and neutron $h_{11/2}$ single-quasiparticle level energies as a function of the γ deformation. The shape of the nucleus and sense of rotation are shown at the top of the figure for specific values of γ that correspond to axially symmetric shapes.

$h_{11/2}$ neutrons favors a collectively rotating oblate shape ($\gamma \sim -60°$). This results because the neutron Fermi surface lies in the upper $h_{11/2}$ midshell. Whether the observed band crossings are due to the alignment of protons or neutrons will thus depend on the degree of γ softness of the nuclei. This may be expressed by the parameter V_{po} which is the energy difference between a prolate and an oblate shape. In the mass $A = 130$ region, $|V_{po}| \leq 1$ MeV, and is calculated to decrease in magnitude as the neutron Fermi surface rises.[2,12] This indicates that the heavier isotopes are more γ soft. However, for ^{135,137}Pm, the magnitude of V_{po} is still large enough to hinder the neutron alignment.

Calculated energy levels e'_μ (Routhians) of the single-quasiparticle states in the rotating frame are shown in Fig. 6. In order to investigate the total energy of the nucleus, a γ-dependent reference has been added to the single-quasiparticle Routhians in accordance to the methods proposed by Frauendorf and May,[1] i.e.,

$$E_{ref}(\omega,\gamma) = \tfrac{1}{2}V_{po}\cos 3\gamma$$

$$- \tfrac{2}{3}\omega^2(\mathcal{J}_0 + \tfrac{1}{2}\omega^2\mathcal{J}_1)\cos^2(\gamma + 30°) . \qquad (5)$$

The Harris parameters are those used in constructing the experimental alignments of Fig. 5. The total Routhian E' for a multiquasiparticle configuration is then given by

$$E'(\omega,\gamma) = \sum_\mu e'_\mu(\omega,\gamma) + E'_{ref}(\omega,\gamma) . \qquad (6)$$

Figure 7 shows such total Routhians plotted vs γ for both one-quasiparticle states and three-quasiparticle states. The calculations were performed at a fixed frequency of $\hbar\omega = 250$ keV, and V_{po} was set to zero. The minimum in the Routhian containing the aligned neutrons occurs at $\gamma \sim -60°$ and is ~ 300 keV lower in energy than that of the aligned-proton configuration; this is neglecting V_{po}, the energy required to drive the core to an oblate $\gamma = -60°$ shape. The calculation thus indicates that if the magnitude of V_{po} is less than 300 keV, the neutron alignment can compete with the proton alignment with an associated shape change to $\gamma \sim -60°$ (oblate collective). However, the magnitude of V_{po} is calculated to be somewhat larger[12] ($V_{po} \sim 800$ keV) than this value for ^{135,137}Pm, and hence the neutron alignment is suppressed. For the heavier ^{139}Pm nucleus, the magnitude of V_{po} is indeed predicted[12] to be less than 300 keV and recent experiments[7] have found a $\Delta J = 1$ sideband built on the $\pi h_{11/2} \otimes (\nu h_{11/2})^2$ configuration at $\gamma \sim -60°$. In addition, a simultaneous alignment of both $h_{11/2}$ protons and $h_{11/2}$ neutrons is observed in the yrast band. The five-quasiparticle band built on the $(\pi h_{11/2})^3 \otimes (\nu h_{11/2})^2$ configuration has a similar shape to the one-quasiproton $\pi h_{11/2}$ band because the presence of the three $h_{11/2}$ quasiprotons overcomes the driving force of the two $h_{11/2}$ neutrons, thus maintaining a near-prolate shape for the nucleus. The double alignment in ^{139}Pm is evident in Fig. 5, where the increase in alignment observed in this nucleus ($\Delta i \sim 14\hbar$) is compared to that observed in the neighboring ^{137}Pm nucleus

($\Delta i \sim 8\hbar$).

B. The sidebands of ^{135,137}Pm

In addition to the decoupled $\pi h_{11/2}$ band observed in ^{137}Pm, two sidebands are seen feeding into the $\tfrac{19}{2}^-$ and $\tfrac{23}{2}^-$ levels. These two bands are believed to be the opposite signatures of a three-quasiparticle structure $\pi[413]\tfrac{5}{2}^+ \otimes (\pi h_{11/2})^2$ as seen[5,6,20] in the neighboring odd-proton nuclei ^{131}La, ^{133}Pr, and ^{135}Pr. In these nuclei, positive parity sidebands built on a $\pi g_{7/2}$ orbital exhibit a low frequency alignment due to the first pair of valence $h_{11/2}$ protons. Such an alignment is not blocked in the positive parity sidebands as is the case in the $\pi h_{11/2}$ yrast bands. One difference for ^{137}Pm is that the one-quasiparticle bands below the band crossing were not observed experimentally. A precise crossing frequency for the alignment of the first pair of valence $h_{11/2}$ protons thus cannot be obtained but can be estimated as $\hbar\omega_c < 0.30$ MeV. This value is consistent with the value of 0.28 MeV predicted by CSM calculations for $\gamma \sim 0°$.

The sidebands in ^{135}Pm were populated only weakly. The band built on the $\tfrac{21}{2}^{(+)}$ state is based on the signature $\alpha = +\tfrac{1}{2}$ component of the $\pi[413]\tfrac{5}{2}^+ \otimes (\pi h_{11/2})^2$ configuration similar to that seen in ^{137}Pm. The band built on the $(\tfrac{19}{2}^+)$ state may be the $\alpha = -\tfrac{1}{2}$ component of this three-quasiproton configuration. However, unlike ^{137}Pm, no connecting $M1$ transitions were observed, and the $E2$ transition energies are similar in both sidebands. The two positive-parity Nilsson levels that lie near the Fermi surface are derived from $g_{7/2}$ and $d_{5/2}$ shell-model states. These levels are near degenerate and thus may mix. Indeed measured $E2/M1$ mixing ratios and $B(M1)/B(E2)$ ratios in the case of ^{131}La imply an admixture of $g_{7/2}$ and $d_{5/2}$ in the sidebands built on the $[413]\tfrac{5}{2}^+$ Nilsson level. The corresponding sidebands observed[7] in the ^{139}Pm nucleus also show this feature of similar transition energies within the bands, unlike ^{137}Pm.

IV. CONCLUSIONS

The systematics of the particle alignments observed in the $\pi h_{11/2}$ bands of the odd-proton ^{133,135,137,139}Pm isotopes have been discussed. The smooth upbend seen in ^{133}Pm becomes sharper in ^{135}Pm, and finally a backbend is observed in ^{137}Pm. All the nuclei show similar crossing frequencies. This alignment is attributed to a pair of protons from the lower $h_{11/2}$ midshell, and the change from upbend to backbend is due to the changing interaction strength between one- and three-quasiproton states as a function of the position of the neutron Fermi surface. The structure of the positive-parity sidebands of the promethium isotopes is also seen to change as a function of the neutron Fermi surface. Competition from the alignment of a pair of neutrons from the upper $h_{11/2}$ midshell was not observed in the ^{135,137}Pm nuclei. An alignment of neutrons would tend to drive the nucleus to an oblate shape. That such neutron alignments are not observed for these isotopes suggests that the prolate-oblate potential energy difference is sufficiently large for these

nuclei to suppress such an alignment, and is in agreement with theoretical predictions. Finally, there is recent evidence for both proton and neutron alignments in the heavier ^{139}Pm isotope, which is predicted to be softer with respect to the γ deformation. A $\Delta J = 1$ band is observed

built on the $\pi h_{11/2} \otimes (\nu h_{11/2})^2$ configuration with $\gamma \sim -60°$.

*Present address: Research Institute of Physics, S 104 05 Stockholm 50, Sweden.

†Present address: Institute of Atomic Energy, Beijing, People's Republic of China.

[1]S. Frauendorf and F. R. May, Phys. Lett. **125B**, 245 (1983).

[2]I. Ragnarsson, A. Sobiczewski, R. K. Sheline, S. E. Larsson, and B. Nerlo-Pomorska, Nucl. Phys. **A233**, 329 (1974).

[3]Y. S. Chen, S. Frauendorf, and G. A. Leander, Phys. Rev. C **28**, 2437 (1983).

[4]G. Andersson, S. E. Larsson, G. Leander, P. Möller, S. G. Nilsson, I. Ragnarsson, S. Åberg, R. Bengtsson, J. Dudek, B. Nerlo-Pomorska, K. Pomorski, and Z. Szymański, Nucl. Phys. **A268**, 205 (1976).

[5]E. S. Paul. C. W. Beausang, D. B. Fossan, R. Ma, W. F. Piel, Jr., N. Xu, and L. Hildingsson, Phys. Rev. Lett. **58**, 984 (1987).

[6]L. Hildingsson, C. W. Beausang, D. B. Fossan, and W. F. Piel, Jr., Phys. Rev. C **33**, 2200 (1986); submitted to Phys. Rev. C.

[7]N. Xu, C. W. Beausang, D. B. Fossan, E. S. Paul, W. F. Piel, Jr., P. K. Weng, J. A. Cizewski, and E. Gülmez, Bull. Am. Phys. Soc. **32**, 1096 (1987); submitted to Phys. Rev. C.

[8]S. Shi, C. W. Beausang, D. B. Fossan, R. Ma, E. S. Paul, W. F. Piel, Jr., P. K. Weng, and N. Xu, Bull. Am. Phys. Soc. **32**, 1095 (1987).

[9]E. S. Paul, C. W. Beausang, D. B. Fossan, R. Ma, W. F. Piel, Jr., P. K. Weng, and N. Xu, Bull. Am. Phys. Soc. **32**, 1095 (1987); Phys. Rev. C **36**, 153 (1987).

[10]A. Zemel, C. Broude, E. Dafni, A. Gelberg, M. B. Goldberg, J. Gerber, G. J. Kumbartzki, and K.-H. Speidel, Nucl. Phys. **A383**, 165 (1982).

[11]M. Müller-Veggian, H. Beuscher, R. M. Lieder, Y. Gono, D. R. Haenni, A. Neskakis, and C. Mayer-Böricke, Z. Phys. A **290**, 43 (1979).

[12]G. A. Leander and W. Nazarewicz, private communication.

[13]C. J. Lister, B. J. Varley, R. Moscrop, W. Gelletly, P. J. Nolan, D. J. G. Love, P. J. Bishop, A. Kirwan, D. J. Thornley, L. Ying, R. Wadsworth, J. M. O'Donnell, H. G. Price, and A. H. Nelson, Phys. Rev. Lett. **55**, 810 (1985).

[14]E. S. Paul, C. W. Beausang, D. B. Fossan, W. F. Piel, Jr., P. K. Weng, and N. Xu, Bull. Am. Phys. Soc. **31**, 1212 (1986).

[15]C. W. Beausang, L. Hildingsson, W. F. Piel, Jr., and D. B. Fossan, Bull. Am. Phys. Soc. **30**, 1264 (1985).

[16]L. Hildingsson, C. W. Beausang, D. B. Fossan, W. F. Piel, Jr., A. P. Byrne, and G. D. Dracoulis, Nucl. Instrum. Methods **A252**, 91 (1986).

[17]R. Bengtsson and S. Frauendorf, Nucl. Phys. **A237**, 139 (1979).

[18]S. M. Harris, Phys. Rev. **138**, B509 (1965).

[19]G. A. Leander, S. Frauendorf, and F. R. May, in *Proceedings of the Conference on High Angular Momentum Properties of Nuclei, Oak Ridge, 1982*, edited by N. R. Johnson (Harwood-Academic, New York, 1983), p. 281.

[20]T. M. Semkow, D. G. Sarantites, K. Honkanen, V. Abenante, L. A. Adler, C. Baktash, N. R. Johnson, I. Y. Lee, M. Oshima, Y. Schutz, Y. S. Chen, J. X. Saladin, C. Y. Chen, O. Dietzsch, A. J. Larabee, L. L. Riedinger, and H. C. Griffin, Phys. Rev. C **34**, 523 (1986).